Journal of Solid State Chemistry **159,** 163–169 (2001)
doi:10.1006/jssc.2001.9145, available online at http://www.idealibrary.com on IDEAL®

# Crystal Structures and Magnetic Properties of New Quaternary Sulfides $BaLn_2MS_5$ ($Ln$ = La, Ce, Pr, Nd; $M$ = Co, Zn) and $BaNd_2MnS_5$

Makoto Wakeshima and Yukio Hinatsu

*Division of Chemistry, Graduate School of Science, Hokkaido University, Sapporo 060–0810, Japan*

Received December 1, 2000; in revised form February 26, 2001; accepted March 15, 2001; published online May 11, 2001

**Crystal structures and magnetic properties are investigated for new quaternary sulfides $BaLn_2TS_5$ ($Ln$ = La, Ce, Pr, Nd; $T$ = Co, Zn) and $BaNd_2MnS_5$. These compounds crystallize in a tetragonal structure (space group *I4mcm*), which is isostructural with $BaLa_2MnS_5$. Their lattice parameters increase monotonically with the sizes of the lanthanide and transition metal. The increase of the *a* values is mainly due to the lanthanide size, and that of the *c* values is due to the transition metal size. In $BaLn_2CoS_5$, the $Co^{2+}$ ions have the unquenched orbital moments. In $BaNd_2MnS_5$, the magnetic anomaly due to the antiferromagnetic ordering of the $Mn^{2+}$ ion, is found at 63 K. Antiferromagnetic orderings for the $Co^{2+}$ ions are observed at ca. 65 K in $BaLn_2CoS_5$ ($Ln$ = La, Ce, Pr, Nd). For $BaNd_2TS_5$ ($T$ = Mn, Co, Zn), the $Nd^{3+}$ ions also show antiferromagnetic behavior below 6 K.** 

## INTRODUCTION

A quaternary manganese sulfide $BaLa_2MnS_5$ crystallizes in a tetragonal structure (space group $I4/mcm$) based on the stacking of $BaMnS_4$ and $La_2S$ layers (1). In the $BaMnS_4$ layer, the Mn ion is bonded to four sulfur ions in a tetrahedral coordination form and these $MnS_4$ tetrahedra link via the Ba ions. Its electrical properties showed an *n*-type semiconductivity. Recently, we investigated the crystal structures and magnetic properties of $BaLn_2MnS_5$ ($Ln$ = La, Ce, and Pr) (2). From their electron paramagnetic resonance spectra, magnetic susceptibilities, and specific heats, the Mn ions were found to be in the $^6S_{5/2}$ state and showed the antiferromagnetic ordering at 58.5 K for $BaLa_2MnS_5$, 62 K for $BaCe_2MnS_5$, and 64.5 K for $BaPr_2MnS_5$. In the succeeding paper, the collinear antiferromagnetic structure of $BaLa_2MnS_5$ was determined through the powder neutron diffraction measurements (3).

In the present study, we have attempted to substitute the $Co^{2+}$ and $Zn^{2+}$ ions for the $Mn^{2+}$ ions, and prepared new quaternary sulfides $BaLn_2MS_5$ ($Ln$ = La, Ce, Pr, Nd; $M$ = Co, Zn). In these compounds, the divalent 3*d* transition elements are expected to occupy the $Mn^{2+}$ tetrahedral sites. The substitution of $Mn^{2+}$ by a diamagnetic $Zn^{2+}$ enables us to investigate the effect of the lanthanide ions on the magnetic properties of these sulfides. Moreover, the sulfides in which the $Mn^{2+}$ ions are substituted by $Co^{2+}$ ions can be expected to show interesting electrical and magnetic properties (4, 5). In this paper, we report the preparation, crystal structures, and magnetic properties of a series of new quaternary sulfides, $BaLn_2MS_5$ and $BaNd_2MnS_5$.

## EXPERIMENTAL

Quaternary sulfides $BaLn_2TS_5$ ($Ln$ = La, Ce, Pr, Nd; $T$ = Co, Zn) and $BaNd_2MnS_5$ were synthesized by a solid-state reaction. Barium sulfide BaS and lanthanide sesquisulfides $Ln_2S_3$ ($Ln$ = La, Ce, Pr, Nd) were prepared by heating $BaCO_3$, $Ln_2O_3$ ($Ln$ = La, Pr, Nd), and $CeO_2$ in a stream of $CS_2/N_2$, which was obtained by bubbling $N_2$ gas through liquid $CS_2$, at 1323 K for 6 h. The stoichiometric mixture of metal sulfides was ground, put into a quartz ampoule, evacuated, and sealed. Then, each ampoule was heated at 1223 K for $BaLn_2TS_5$ ($T$ = Co, Zn) and at 1273 K for $BaNd_2MnS_5$ for 2 days with regrinding at intervals.

Powder X-ray diffraction measurements were carried out using a Rigaku RINT2200 diffractometer with graphite-monochromatized Cu$K\alpha$ radiation at room temperature. An angular range $2\theta$ from 10 to 120° was scanned in steps of 0.02° with a step time 5 s. The program RIETAN97 (6) was used for refinements of crystal structures by the Rietveld method. A pseudo-Voigt profile function was applied to describe the peak shape.

The magnetic susceptibility measurements were carried out using a SQUID magnetometer (Quantum Design, MPMS-5S). The temperature dependence of the susceptibilities was measured under an applied magnetic field of 0.1 T after cooling down to 2 K in a zero field (ZFC) and was measured on cooling under the field (FC) of 0.1 T. The magnetic susceptibility data were corrected for the diamagnetic contribution of the atomic cores (7).



0022-4596/01 $35.00

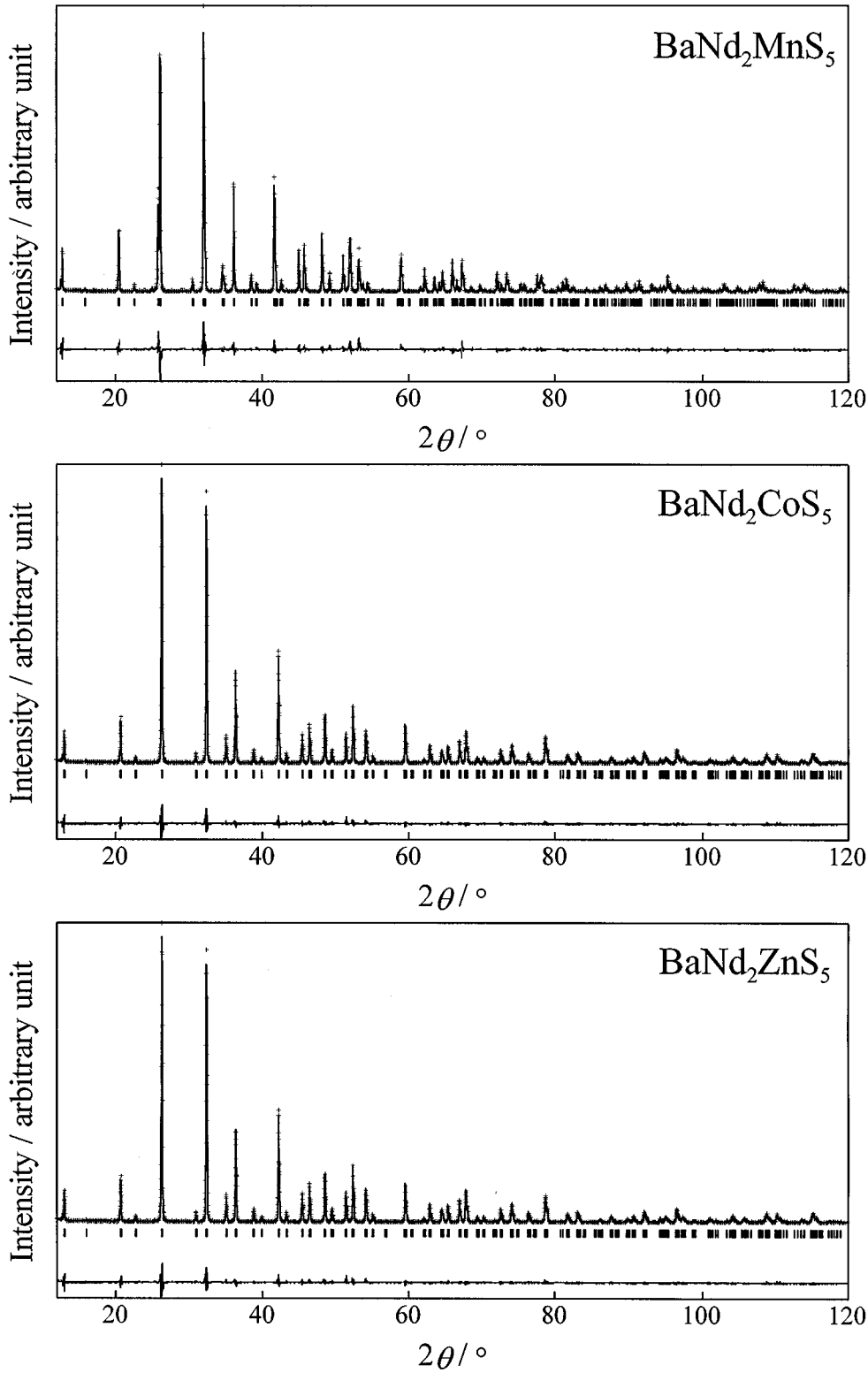


**FIG. 1.** Powder X-ray diffraction patterns and Rietveld refinements for $BaNd_2TS_5$ ($T$ = Mn, Co, Zn). In each case, the bottom trace is a plot of the difference between (+) observed and (—) calculated intensities. All allowed Bragg reflections are shown by vertical lines.

**TABLE 1**
**Lattice and Positional Parameters of Ba$Ln_2TS_5$ ($Ln$ = La, Ce, Pr, Nd; $T$ = Mn, Co, Zn)**

| | $BaNd_2MnS_5$ | $BaLa_2CoS_5$ | $BaCe_2CoS_5$ | $BaPr_2CoS_5$ | $BaNd_2CoS_5$ | $BaLa_2ZnS_5$ | $BaCe_2ZnS_5$ | $BaPr_2ZnS_5$ | $BaNd_2ZnS_5$ |
|---|---|---|---|---|---|---|---|---|---|
| $a$/Å | 7.8583(1) | 7.9636(1) | 7.8829(1) | 7.8473(1) | 7.8134(1) | 7.9823(1) | 7.9102(1) | 7.8719(1) | 7.8394(1) |
| $c$/Å | 13.7807(2) | 13.6189(2) | 13.5988(2) | 13.5790(2) | 13.5586(2) | 13.6708(2) | 13.6579(2) | 13.6327(2) | 13.6131(1) |
| $x(Ln)$ | 0.1613(3) | 01.1632(1) | 0.1624(3) | 0.1631(3) | 0.1630(3) | 0.1623(3) | 0.1620(3) | 0.1621(4) | 0.1622(3) |
| $x$(S(2)) | 0.1536(10) | 0.1481(4) | 0.1488(10) | 0.1477(9) | 0.1482(9) | 0.1510(9) | 0.1505(9) | 0.1499(10) | 0.1497(9) |
| $z$ (S(2)) | 0.6329(6) | 0.6375(2) | 0.6364(6) | 0.6359(6) | 0.6350(6) | 0.6376(6) | 0.6359(6) | 0.6346(7) | 0.6343(6) |
| $R_I$/% | 3.26 | 3.02 | 3.28 | 2.47 | 2.32 | 3.17 | 2.89 | 2.11 | 1.91 |
| $R_F$/% | 2.01 | 1.93 | 1.80 | 1.66 | 1.41 | 2.02 | 1.53 | 1.45 | 1.16 |
| $R_{wp}$/% | 12.57 | 13.43 | 14.09 | 13.33 | 11.14 | 11.63 | 13.44 | 13.90 | 11.33 |

*Note.* $R_I = \sum|I_{obs} - I_{cal}|/\sum I_{obs}$, $R_F = \sum|I_{obs}^{1/2} - I_{cal}^{1/2}|/\sum I_{obs}^{1/2}$, $R_{wp} = [\sum w(y_{obs} - y_{cal})^2/\sum w y_{obs}^2]^{1/2}$. Ba is located in the 4$a$ $(0,0,\frac{1}{4})$ site, $Ln$ in the 8 h $(x, x+\frac{1}{2}, 0)$ site, $T$ in the 4$b$ $(0,\frac{1}{2},\frac{1}{4})$ site, S(1) in the 4$c$ $(0,0,0)$ site, and S(2) in the 16$l$ $(x, x+\frac{1}{2}, z)$ site.

## RESULTS AND DISCUSSION

### *Crystal Structures*

Quaternary sulfides Ba$Ln_2TS_5$ ($Ln$ = La, Ce, Pr, Nd; $T$ = Co, Zn) and $BaNd_2MnS_5$ were obtained as single phases. Their powder X-ray diffraction patterns were confirmed to be similar to those for the Ba$Ln_2MnS_5$ ($Ln$ = La, Ce, Pr). Their diffraction patterns were indexed on a tetragonal cell, which was isostructural with Ba$Ln_2MnS_5$ (space group $I4/mcm$), with four chemical formulas per unit cell. Figure 1 shows the observed and calculated diffraction patterns for $BaNd_2TS_5$ ($T$ = Mn, Co, Zn). For the Rietveld analysis, three positional parameters of $BaLa_2MnS_5$ (2) were used as the initial positional parameters. The initial lattice parameters were calculated by the least-squares method. The refined lattice parameters and atomic positions of Ba$Ln_2TS_5$ ($Ln$ = La, Ce, Pr, Nd; $T$ = Co, Zn) and $BaNd_2MnS_5$ are given in Table 1. Barium, lanthanide, and manganese (cobalt, zinc) cations are located in 4$a$ $(0,0,\frac{1}{4})$, 8$h$ $(x, x+\frac{1}{2}, 0)$, and 4$b$ $(0,\frac{1}{2},\frac{1}{4})$ sites, respectively. Sulfur anions occupy two different sites, S(1) and S(2) in 4$c$ $(0,0,0)$ and 16$l$ $(x, x+\frac{1}{2}, z)$, respectively. The schematic structure of Ba$Ln_2TS_5$ ($Ln$ = La, Ce, Pr, Nd; $T$ = Mn, Co, Zn) is illustrated in Fig. 2. The Ba$TS_4$ layers and $Ln$S layers, which

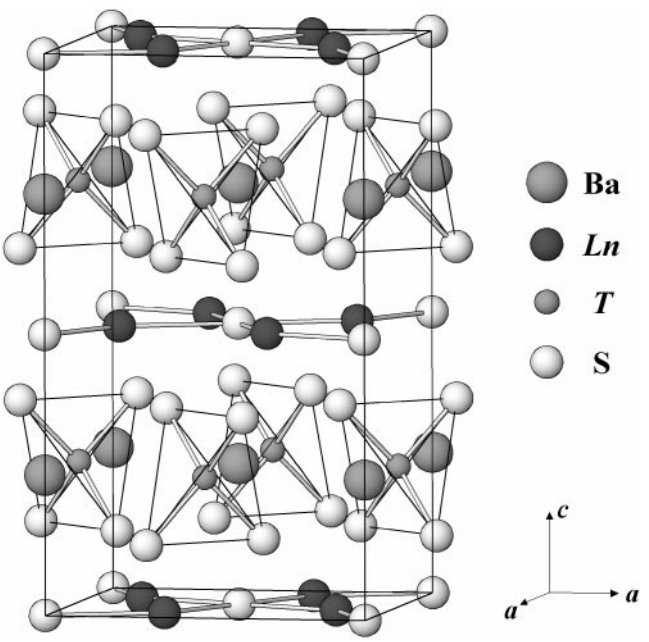


**FIG. 2.** The schematic structure of $Ba_2LnTS_5$ ($Ln$ = La, Ce, Pr, Nd; $T$ = Mn, Co, Zn).

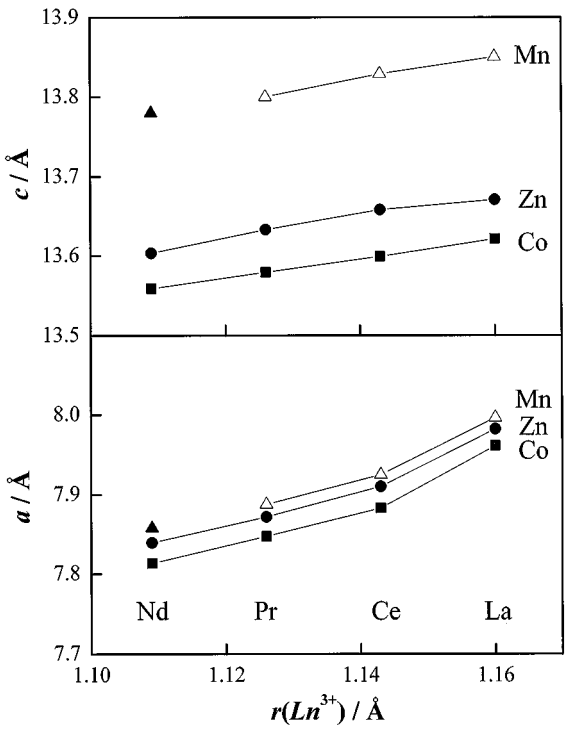


**FIG. 3.** Lattice parameters as a function of $Ln^{3+}$ ionic radius. Data in this work and in Ref. (2) are represented by open and closed markers, respectively.

**TABLE 2**
**Bond Lengths for Ba$Ln_2TS_5$ ($Ln$ = La, Ce, Pr, Nd; $T$ = Mn, Co, Zn)**

| | $BaNd_2MnS_5$ | $BaLa_2CoS_5$ | $BaCe_2CoS_5$ | $BaPr_2CoS_5$ | $BaNd_2CoS_5$ | $BaLa_2ZnS_5$ | $BaCe_2ZnS_5$ | $BaPr_2ZnS_5$ | $BaNd_2ZnS_5$ |
|---|---|---|---|---|---|---|---|---|---|
| Bond Length $r$/Å | | | | | | | | | |
| Ba–S(1) × 2 | 3.445 | 3.405 | 3.400 | 3.395 | 3.390 | 3.418 | 3.415 | 3.408 | 3.403 |
| Ba–S(2) × 8 | 3.386(3) | 3.405(2) | 3.382(4) | 3.375(4) | 3.365(4) | 3.402(4) | 3.389(5) | 3.385(6) | 3.376(3) |
| *Ln*–S(1) × 2 | 2.947(1) | 2.981(1) | 2.954(1) | 2.937(1) | 2.925(1) | 2.991(1) | 2.965(1) | 2.950(1) | 2.938(1) |
| *Ln*–S(2) × 2 | 2.757(6) | 2.833(4) | 2.805(7) | 2.795(7) | 2.776(8) | 2.825(7) | 2.801(9) | 2.783(10) | 2.774(7) |
| *Ln*–S(2) × 4 | 3.081(8) | 3.109(3) | 3.078(8) | 3.060(7) | 3.046(7) | 3.130(7) | 3.093(7) | 3.067(9) | 3.055(7) |
| *T*–S(2) × 4 | 2.345(6) | 2.265(4) | 2.268(7) | 2.245(7) | 2.259(8) | 2.296(7) | 2.294(9) | 2.289(10) | 2.288(7) |

are perpendicular to the $c$ axis, are stacked alternately. The Ba ions are coordinated by eight nearest-neighbor sulfur ions S(2) and two next-nearest-neighbor sulfur ions S(1). The $Ln$ ions have eight sulfur neighbors.

The lattice parameters as a function of the lanthanide ionic radius referred from Shannon's ionic radii (8) are shown in Fig. 3. Those of Ba$Ln_2MnS_5$ ($Ln$ = La, Ce, Pr) reported in Ref. (2) are also shown in Fig. 3. Both the $a$ and $c$ parameters increase with the lanthanide ionic radius and the variation of the $a$ parameters is steeper than that of the $c$ parameters. Furthermore, these parameters increase with the transition metal ionic radius (0.66 Å for $Mn^{2+}$, 0.58 Å for $Co^{2+}$, and 0.60 Å for $Zn^{2+}$) and the variation of the $c$ parameters is larger than that of the $a$ parameters. Some selected bond lengths are listed in Table 2 and their variation against the $Ln^{3+}$ ionic radius is plotted in Fig. 4. The Ba–S and $Ln$–S lengths increase monotonously with the size of the $Ln^{3+}$ ions, while the Mn–S, Co–S, and Zn–S lengths are almost constant within the experimental errors for variation of the $Ln^{3+}$ ionic radius.

## *Magnetic Properties*

*Magnetic susceptibilities of Ba$Ln_2ZnS_5$ ($Ln$ = Ce, Pr, Nd).* The reciprocal molar magnetic susceptibilities of Ba$Ln_2ZnS_5$ ($Ln$ = Ce, Pr, Nd) are shown as a function of temperature in Fig. 5. In these compounds, only the lanthanide ions are magnetic. The effective magnetic moments $\mu_{eff}$ per mole of the lanthanide ion are determined to be 2.551(2) $\mu_B$ for $BaCe_2ZnS_5$, 3.666(2) $\mu_B$ for $BaPr_2ZnS_5$, and 3.655(1) $\mu_B$ for $BaNd_2ZnS_5$ by applying the Curie–Weiss law ($\chi = C/(T-\theta)$) to the reciprocal susceptibility vs temperature curve in the high temperature region (150 K $\leq T \leq$ 300 K). These calculated moments agree well with the magnetic moments of free trivalent lanthanide ions (2.54 $\mu_B$ for $Ce^{3+}$, 3.58 $\mu_B$ for $Pr^{3+}$, 3.62 $\mu_B$ for $Nd^{3+}$).

The convex curve of $BaCe_2ZnS_5$ at lower temperatures should be attributable to the contribution of the crystal field effect. Only the $BaNd_2ZnS_5$ compound shows a magnetic anomaly at low temperatures. The inset of Fig. 5 shows the magnetic susceptibility of $BaNd_2ZnS_5$ below 10 K. It shows a maximum at 3.9 K and indicates that the $Nd^{3+}$ ion is in an antiferromagnetic state below this temperature. Since the $Ce^{3+}$ ions are capable of showing magnetic interactions at lower temperatures, the $BaCe_2ZnS_5$ compound should also show some magnetic transition at furthermore lower temperatures.

*Magnetic susceptibility of $BaNd_2MnS_5$.* Figure 6 shows the temperature dependence of the molar magnetic susceptibilities of $BaNd_2MnS_5$. No divergence between the ZFC and FC magnetic susceptibilities is observed. The susceptibility of $BaNd_2MnS_5$ indicates an antiferromagnetic transition at $T_{N1}$ ($\sim$ 4.7 K) and a magnetic anomaly at $T_{N2}$ ($\sim$ 63 K). This antiferromagnetic transition should be attributable to the antiferromagnetic ordering of the $Nd^{3+}$ ions, because similar magnetic transition at the nearly same temperature has been observed in $BaNd_2ZnS_5$ (see Fig. 5).

Figure 7 shows the first derivative of the magnetic susceptibility of $BaNd_2MnS_5$ in the neighborhood of $T_{N2}$. The results for Ba$Ln_2MnS_5$ ($Ln$ = La, Ce, Pr) (2) are also shown in Fig. 7. The magnetic anomaly found for $BaNd_2MnS_5$ at $\sim$ 63 K is quite similar to those reported for Ba$Ln_2MnS_5$ ($Ln$ = La, Ce, Pr). From the magnetic susceptibility and the specific heat measurements, the $Mn^{2+}$ ions were found to be in the antiferromagnetic state below 58.5 K for $BaLa_2MnS_5$, 62 K for $BaCe_2MnS_5$, and 64.5 K for $BaPr_2MnS_5$ (2). Therefore, the anomaly found at $T_{N2}$ (63 K) in $BaNd_2MnS_5$ should be due to the antiferromagnetic interactions between $Mn^{2+}$ ions.

The inset of Fig. 6 shows the reciprocal magnetic susceptibility vs temperature curve for $BaNd_2MnS_5$ in the 150–300 K temperature range. The Curie–Weiss law holds in this temperature range, which yields the Weiss constant $\theta = -76.8(1)$ K and the Curie constant $C = 7.588(3)$ emu mol$^{-1}$ K$^{-1}$ for one formula unit. The spectrum of $BaNd_2MnS_5$, taken from electron paramagnetic resonance (EPR) measurement at room temperature, is very similar to that of $BaLa_2MnS_5$ in Ref. (2), and the $g$ value is calculated

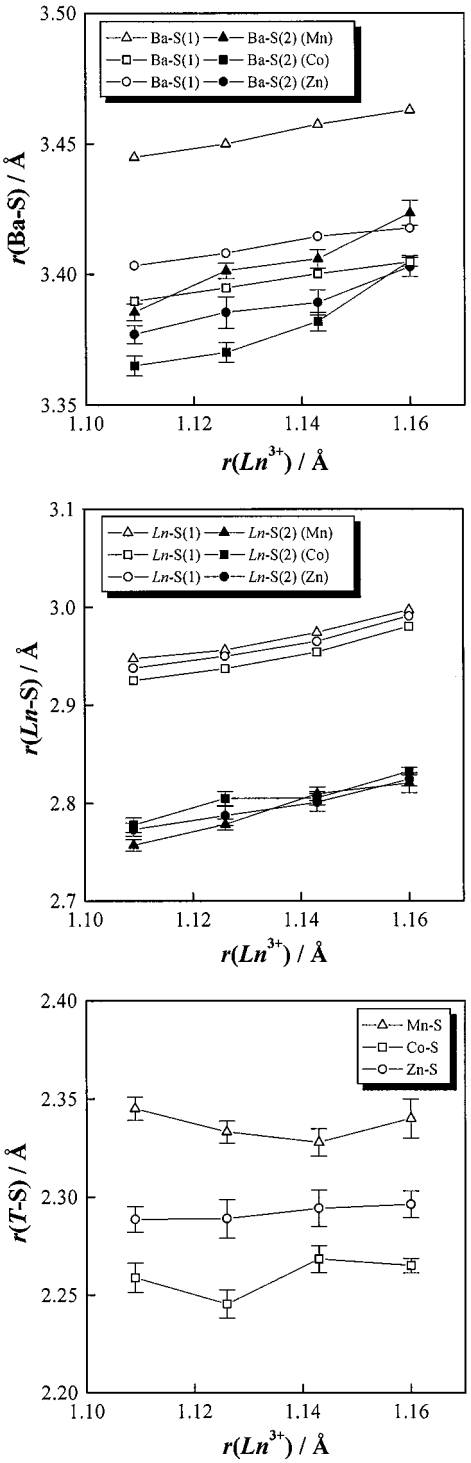


**FIG. 4.** Variation of the bond lengths as a function of $Ln^{3+}$ ionic radius.

to be 2.00. This result means that the Mn ion is in the $^6S_{5/2}$ state without an orbital moment contribution, and its effective magnetic moment $\mu_{\text{eff}}$ is 5.92 $\mu_B$. The total effective magnetic moment of $BaNd_2MnS_5$ is represented by the

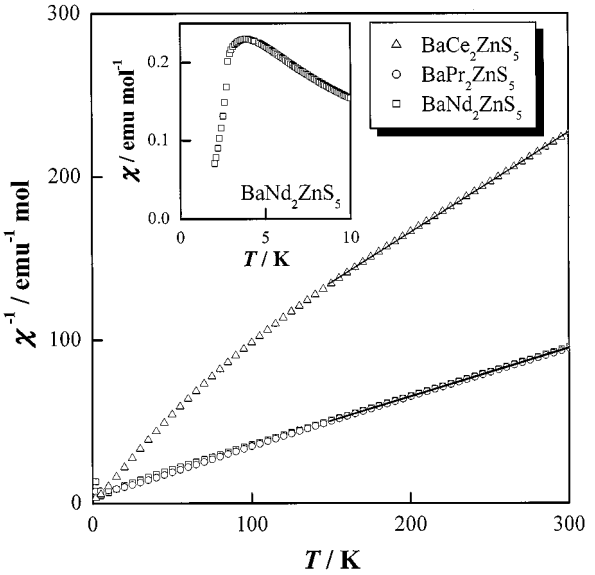


**FIG. 5.** Temperature dependence of the reciprocal magnetic susceptibility $\chi^{-1}$ of $BaLn_2ZnS_5$ ($Ln$ = Ce, Pr, Nd). Straight lines represent the Curie–Weiss law fittings (see text). The inset shows $\chi$ of $BaNd_2ZnS_5$ below 10 K.

equation $\mu_{\text{eff}}(\text{total})^2 = \mu_{\text{eff}}(Mn^{2+})^2 + 2\mu_{\text{eff}}(Nd^{3+})^2$. Assuming that the effective moment of $Mn^{2+}$ is 5.92 $\mu_B$, the moment of $Nd^{3+}$ is estimated to be 3.59 $\mu_B$, which is in good agreement with the value of a free $Nd^{3+}$ ion (3.62 $\mu_B$).

*Magnetic susceptibilities of $BaLn_2CoS_5$ ($Ln$ = La, Ce, Pr, Nd).* Figure 8 shows the temperature dependence of the magnetic susceptibilities of $BaLa_2CoS_5$. An antiferromagnetic transition is found at 60 K. From the fitting of

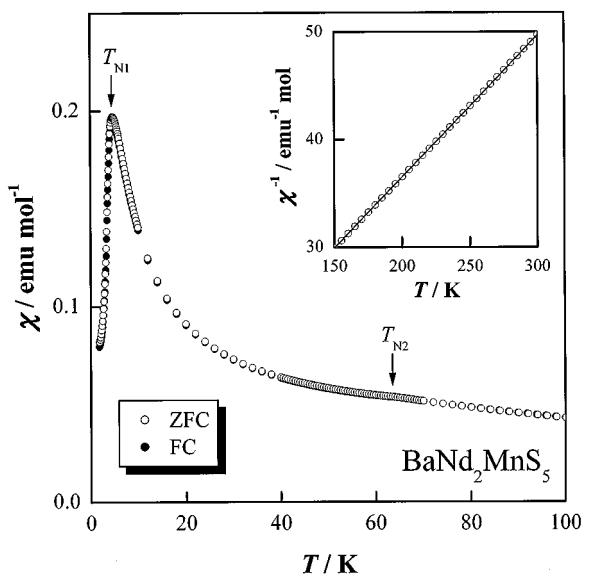


**FIG. 6.** Temperature dependence of the magnetic susceptibility $\chi$ of $BaNd_2MnS_5$. The inset shows $\chi^{-1}$ in the temperature range between 150 and 300 K. A straight line represents the Curie–Weiss law fitting.

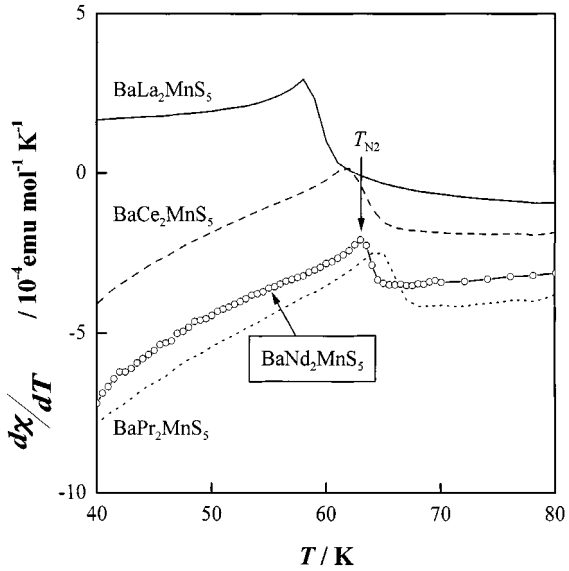


**FIG. 7.** The first derivatives of the magnetic susceptibilities of $BaLn_2MnS_5$ ($Ln$ = La, Ce, Pr, Nd) in the neighborhood of $T_{N2}$.

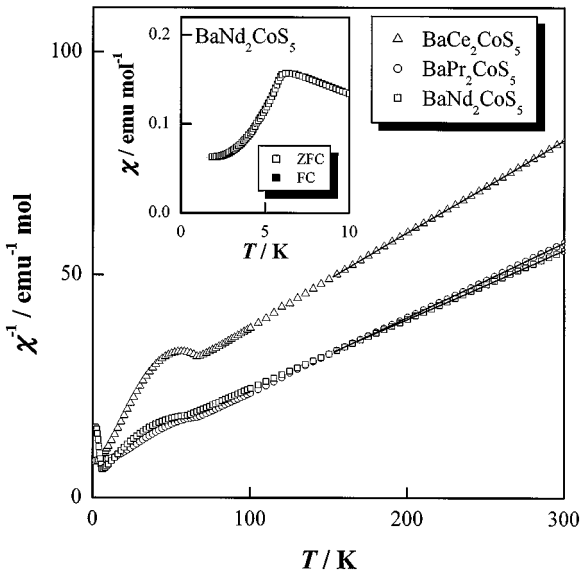


**FIG. 9.** Temperature dependence of the reciprocal magnetic susceptibilities $\chi^{-1}$ of $BaLn_2CoS_5$ ($Ln$ = Ce, Pr, Nd). Straight lines represent the Curie–Weiss law fittings. The inset shows $\chi$ of $BaNd_2CoS_5$ below 10 K.

the Curie–Weiss law the effective magnetic moment of $Co^{2+}$ and a Weiss constant are estimated to be 4.857(2) $\mu_B$ and $-$ 66.4(2) K, respectively. This moment is larger than the value (3.87 $\mu_B$) calculated from the "spin–only" state ($S = 3/2$) of $d^7$ electronic configuration and is smaller than the value (6.63 $\mu_B$) calculated by taking into account the contribution of the spin–orbit interaction. This result indicates that the ground state of $Co^{2+}$ has an unquenched orbital moment.

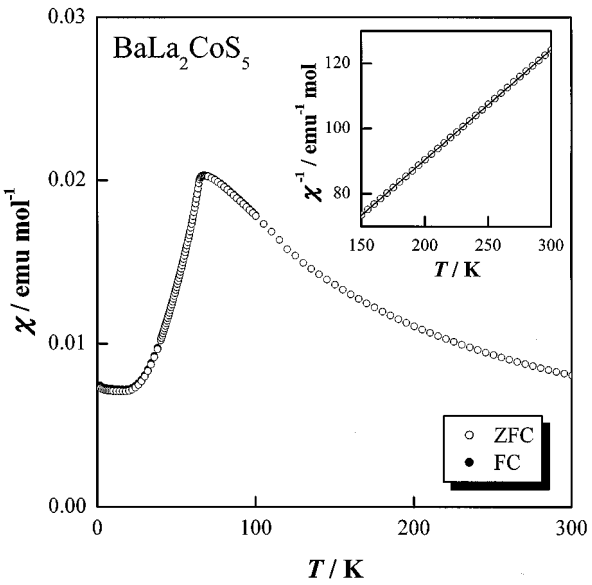


**FIG. 8.** Temperature dependence of the magnetic susceptibility $\chi$ of $BaLa_2CoS_5$. The inset shows $\chi^{-1}$ in the temperature range between 150 and 300 K. A straight line represents the Curie–Weiss law fitting.

Figure 9 shows the reciprocal magnetic susceptibilities of $BaLn_2CoS_5$ ($Ln$ = Ce, Pr, Nd) as a function of temperature. In all the susceptibilities, the magnetic anomalies are found around 65 K and they should be attributable to the antiferromagnetic couplings of the $Co^{2+}$ ions, because a clear antiferromagnetic transition has been observed for $BaLa_2CoS_5$ (La: diamagnetic) at nearly the same temperature (see Fig. 8). In order to determine the Néel temperatures of the $Co^{2+}$ ions, the first derivatives of the magnetic susceptibility of $BaLn_2CoS_5$ ($Ln$ = La, Ce, Pr, Nd) are calculated in the temperature range from 40 to 80 K, and they are shown in Fig. 10. The $Co^{2+}$ ions were found to be in the antiferromagnetic state below 63.5 K for $BaLa_2CoS_5$, 65 K for $BaCe_2CoS_5$, 65 K for $BaPr_2CoS_5$, and 58.5 K for $BaNd_2CoS_5$. For $BaNd_2CoS_5$, another antiferromagnetic ordering occurs below 6.7 K, as shown in the inset of Fig. 9. This ordering should be due to the antiferromagnetic coupling of the $Nd^{3+}$ ions, in analogy with the cases of $BaNd_2ZnS_5$ and $BaNd_2MnS_5$. The magnetic susceptibilities of these compounds obey a Curie–Weiss law at high temperatures. In the $BaLn_2ZnS_5$ compounds, the effective magnetic moment of the $Ln$ ion is very close to that of a free $Ln$ ion. On the assumption that the moment of the $Ln$ ion in the $BaLn_2CoS_5$ compounds also agrees with that of a free $Ln$ ion, the effective magnetic moment of $Co^{2+}$ is calculated to be 5.05 $\mu_B$ for $BaCe_2CoS_5$, 4.79 $\mu_B$ for $BaPr_2CoS_5$, and 5.03 $\mu_B$ for $BaNd_2CoS_5$, indicating that the orbital moments of $Co^{2+}$ ions are not quenched.

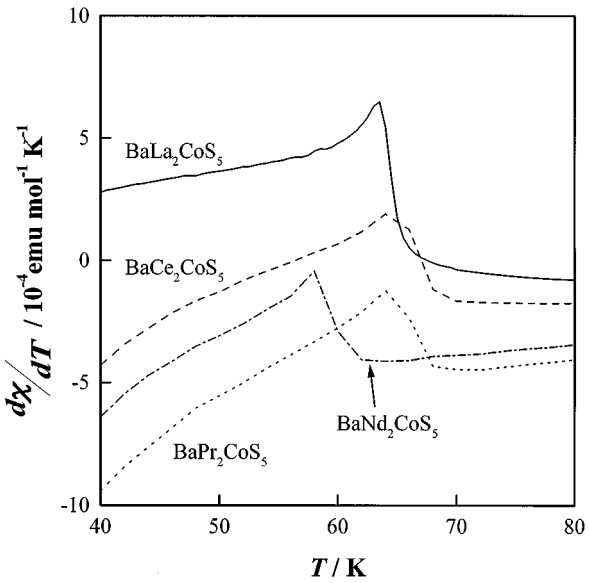


**FIG. 10.** The first derivatives of the magnetic susceptibility of $BaLn_2CoS_5$ ($Ln$ = La, Ce, Pr, Nd) in the temperature range between 40 and 80 K.

## SUMMARY

New quaternary sulfides with a tetragonal structure (space group: *I*4*mcm*), $BaLn_2MS_5$ ($Ln$ = La, Ce, Pr, Nd; $M$ = Co, Zn) and $BaNd_2MnS_5$ were synthesized. The lattice parameters of $a$ increase mainly with the size of the lanthanide ions, and those of $c$ increase with the transition metal size. Magnetic susceptibility measurements show that the $Mn^{2+}$, $Co^{2+}$, and $Nd^{3+}$ ions in these $BaLn_2MS_5$ ($Ln$ = La, Ce, Pr, Nd; $M$ = Mn, Co, Zn) are in the antiferromagnetic states below 63, $\sim$65, and 6 K, respectively.

## REFERENCES

1. H. Masuda, T. Fujino, N. Sato, and K. Yamada, *J. Solid State Chem.* **146,** 336 (1999).
2. M. Wakeshima and Y. Hinatsu, *J. Solid State Chem.* **163,** 330 (2000).
3. M. Wakeshima, Y. Hinatsu, K. Oikawa, Y. Shimojo, and Y. Morii, *J. Mater. Chem.* **10,** 2183 (2000).
4. L. S. Martinson, J. W. Schweitzer, and N. C. Baenziger, *Phys. Rev. B* **54,** 11265 (1996).
5. N. Nakayama, K. Kosuge, S. Kachi, T. Shinjo, and T. Takada, *J. Solid State Chem.* **33,** 351 (1980).
6. F. Izumi, *in* "The Rietveld Method" (R. A. Young, Ed.), Chap. 13. Oxford University Press, Oxford, 1995.
7. L. N. Mulay and E. A. Boudreaux (Eds.), "Theory and Applications of Molecular Diamagnetism." Wiley-Interscience, New York, 1976.
8. R. D. Shannon, *Acta Crystallogr., Sect. A: Found. Crystallogr.* **32,** 751 (1976).